Airborne and Spaceborne Cloud Radar Designs

Fuk Li, Eastwood Im, Stephen Durden, William Wilson

Jet Propulsion Laboratory
California Institute of Technology
Pasadena, CA 91109, USA
T: (818) 354-2849 F: (818) 393-5285 EMail: fuk_li@radar_email.jpl.nasa.gov

ABSTRACT

This paper presents some crucial design parameters and a strawman system design for a nadir-looking, 94-GHz spaceborne cloud profiling radar. This sensor is expected to provide cloud measurements at vertical resolution of 500 m and with a minimum detectable cloud reflectivity of slightly better than -30 dBZ. The radar design is intended to be accommodated by a spacecraft with limited resources. It uses a 2-m antenna and an extended interaction amplifier (EIA) that are readily available in either ground-based and airborne applications. For space application, improvements in the EIA lifetime and space qualification will be required. For various reasons, the spaceborne cloud radar system development is expected to be greatly benefited by the implementation of an aircraft cloud radar instrument.

1. INTRODUCTION

An essential component of the Earth's energy budget is the three-dimensional distribution of radiative and latent heating and cooling in the atmosphere. To derive these quantities, it is necessary to know the global, three-dimensional distributions of clouds and precipitation. Unfortunately, information on the distribution of vertical cloud structure, which is a crucial input to the radiation budget and the atmospheric water vapor distribution, is not available from existing or planned spaceborne remote-sensing instruments.

A recent report by the World Climate Research Program (WCRP, 1994) has documented the potentials of acquiring the near-global cloud measurements with a spaceborne millimeter-wave radar. This paper investigates the design issues associated with such a system and describes a strawman cloud radar design that will meet the scientific needs. In particular, we will discuss the radar frequency selection, the control of surface clutter contamination and its implications on antenna and transmit pulse design, the tradeoffs between sensitivity, spaceborne resource requirements, and technological readiness of the various radar subsystems. The expected performance and spacecraft resource consumption for such system will also be summarized. We have also developed a similar design concept for an airborne cloud profiling radar. The additional design issues associated with wide system dynamic range and Doppler measurements will also be summarized.

2. SPACEBORNE CLOUD RADAR DESIGN ISSUES

We expect that the mission that will carry such a cloud profiling radar will be small to moderate in scale. Therefore, we have assumed a corresponding set of modest spacecraft resources for the cloud radar design. The spacecraft is assumed to operate at a 400-km, circular orbit. This section will discuss several key design issues associated with a spaceborne cloud radar.

2.1 Frequency Selection

Based on the cloud radar reflectivity and our assessment of technology readiness for spaceborne radar components, the frequency range of 35 to 100 GHz is potentially suitable for the cloud radar. A performance comparison was made for a radar system that operates at 35 GHz and one at 94 GHz. To obtain a valid comparison, however, the following assumptions were used in this comparison study:

1. The radar will operate at only one frequency.
2. Same antenna aperture size is used for both systems.
3. Same vertical and along-track integrated resolution are used for both systems.
4. Based on the assessment of the available radar technology, a peak transmit power of 1 KW was adopted for both frequencies.
5. DC-to-RF power conversion efficiencies for the transmitter of 30% at 35 GHz and 12% at 94 GHz are adopted.
6. Average DC power consumed by both systems is the same.
7. 94 GHz system noise temperature is 2 dB larger than at 35 GHz.

With these assumptions, the ratio of the signal-to-noise ratios at the two frequencies is

$$\frac{S_{94}}{S_{35}} \approx \left(\frac{\eta_{94}}{\eta_{35}}\right)^{1/2} \frac{|K_{94}|^2}{|K_{35}|^2} \left(\frac{94}{35}\right)^4 \left(\frac{T_{35}}{T_{94}}\right)\left(\frac{L_{35}}{L_{94}}\right)^2 \quad (1)$$

where η is the DC to RF power efficiency; $|K|^2$ is the dielectric factor of liquid water; T is the system noise temperature; and L is the atmospheric loss due to cloud absorption. This expression is valid for $S_{94}, S_{35} \ll 1$, which will be the case for weak cloud echoes. Using values based on the above assumptions, this ratio is:

$$\frac{S_{94}}{S_{35}} \approx + 12.5 - 2(L_{94} - L_{35}) \text{ dB} \quad (2)$$

where L_{94} and L_{35} are the cloud absorption in dB. Thus, the 94-GHz system is approximately 12 dB more sensitive than the 35-GHz system in detecting the layers near the cloud top, where the cloud absorption is small. As the radar signal continues to penetrate through the cloud column, the signal will be attenuated, and the maximum depth that the signal can penetrate will depend on the cloud water density, as well as the cloud absorption. At a given frequency and by assuming homogeneity of the clouds, the maximum measurable cloud depth (Δd_{max}) can be defined as:

$$\Delta d_{max} = \frac{Z - Z_{min}}{2\alpha} \text{ km} \quad (3)$$

where α is the cloud attenuation (in dB/km), Z is the actual cloud reflectivity (in dB), and Z_{min} is the minimum detectable cloud reflectivity (see Eq. (6)). In this study, α was assumed to be $0.75M$ at 35 GHz and $3.0M$ at 94 GHz, where M is the liquid water content (in g/m^3). These values are in agreement with Rayleigh scattering calculations and with radiometer observations. Following Atlas (1964), the cloud reflectivity is taken to be $Z \approx 0.048M^2$, which can be applied to both frequencies by assuming Rayleigh scattering.

With a DC power of 225 W and a 2-m antenna, the minimum detectable reflectivity, Z_{min}, with no cloud attenuation, is -32.5 dBZ at 94 GHz (see Table 2). The corresponding Z_{min} at 35 GHz according to Eq. (2) is approximately -19 dBZ. Using the assumed attenuation and reflectivity values, the maximum measurable cloud depths are plotted as a function of both Z and M in Fig. 1. For clouds of lower water content, the 94-GHz radar has superior performance. Clouds with water content less than ~0.5 g/m^{-3} cannot be detected by the 35-GHz system. For clouds with $M > 0.75$ g/m^{-3} ($Z \approx -15$ dBZ), the 35-GHz radar is better because of less absorption. As such, the 94-GHz frequency appears to be a better system choice for overall cloud measurements. 94 GHz is also preferable for ice clouds, which have small attenuation.

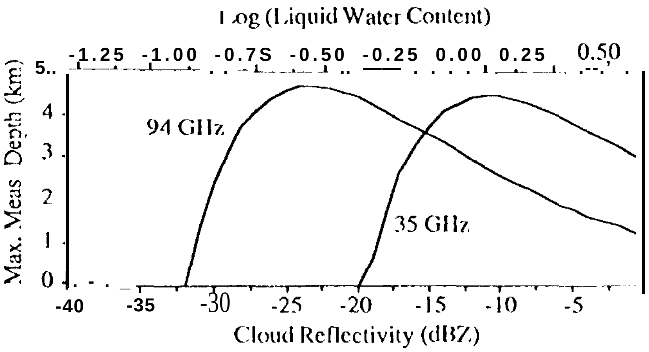

Figure 1, Maximum measurable cloud depth at 35 and 94 GHz vs. cloud reflectivity.

2.2 Surface Clutter Contamination Concerns

With the downward radar viewing geometry and the fact that the Earth's surface is a much stronger scatterer than the cloud, the undesired surface returns must be kept substantially below the cloud reflected signal to extract accurate information of the cloud. One potential path that the surface returns from previous pulse transmissions can "leak" into the cloud return is through the antenna sidelobes. To calculate the required antenna sidelobe level that must be achieved to minimize the surface contaminations, we adopted a set of surface (land and ocean) radar back scatter cross sections versus incidence angles (Ulaby and Dobson 1988; Ulaby, *et.al.* 1982). With these adopted surface backscatter characteristics, the required antenna far-out sidelobes (> 15° from boresight) were computed to be < 50 dB and the required near-in sidelobes to be < -25 dB. For an off-nadir viewing geometry, the near-in antenna sidelobes must be <-50 dB to eliminate surface contamination from the same pulse Transmission.

Another potential route for surface contamination is the sidelobes associated with the transmitted pulses. For example, a common approach to achieve higher signal-to-noise ratio in a radar system is by phase-coding (such as linear FM) a long radar pulse and by subsequent pulse compression of the received radar echoes. However, this approach typically results in pulse compression sidelobes that contaminate the cloud echoes from the surface return. Based on our backscatter model, the required sidelobe levels for two different vertical resolutions desired for the cloud radar were calculated in Fig. 2. It shows that the required pulse compression sidelobe level is at least 85 dB. We believe that practical implementation of a pulse compression scheme that satisfies such a severe requirement is beyond the present state-of-the-art (Tanner *et.al.*, 1993). One, therefore, will be required to use a traditional short, uncoded pulse approach, which requires a correspondingly higher peak transmitter power. Even in this case, one should be careful in controlling the rise/fall time of the transmit pulse to prevent any leakage beyond the desired pulse length.

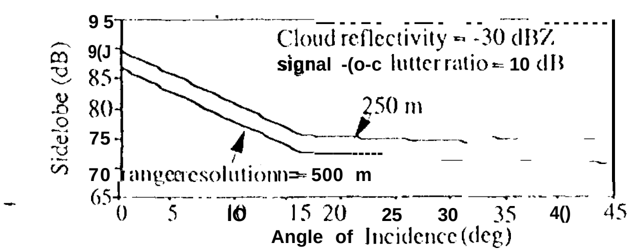

Figure 2. Required compression sidelobe level vs. incidence angle.

2.3 Antenna Size and Scanning

The antenna diameter is limited by the satellite constraints. We have considered a 2-m and a 4-m diameter antenna designs. The 4-m antenna provides better horizontal resolution and signal-to-noise performance. However, it is heavier, requires more "real-estate", creates large blockage for other nadir-viewing instruments, and its deployment would add complexity to the instrument. The less complicated 2-m antenna can be more easily accommodated by the spacecraft and, as shown in Section 3, also meet the performance requirements.

A scanning antenna would provide better spatial coverage; however, it was not considered because of the ground contamination through the antenna sidelobes, as noted above.

3. SPACEBORNE CLOUD RADAR STRAWMAN DESIGN

Given the science and design considerations discussed above, a strawman design for a cloud profiling radar consistent with a small- to moderate mission was constructed. Table I shows the strawman system parameters and the expected spacecraft resource consumption for this radar.

Frequency	94 GHz
Antenna:	
Diameter	2111
Peak gain	63.4 dBi
3-dB beamwidth	0.11°
Near-sidelobe level	<-25 [ill
Far-sidelobe level	< -55 dB
EIA-based transmitter:	
Peak power	1 KW
Power conversion efficiency	12%
Transmitted signal:	
Pulse width	3.33 μsec
Signal bandwidth	300 KHz
Pulse repetition frequency	4250
Transmit duty cycle	1.42%
Transmit path loss	2 [lll
Receiver bandwidth	360 KHz
Receive path loss	3 dB
Receiver noise figure	2 dB
Ave. output data rate (12-bit sampling)	2.1 Kbps
Ave. S/C power	225 W ± 40%
Mass	108 Kg ± 30%
Volume:	
Antenna in stow position	2 m × 2 m × 1 m
Radar electronics	1 m x 0.6 m x 0.3 m

Table I. The preliminary estimates of the system parameters for a spaceborne cloud radar design.

The single-pulse cloud signal-to-noise ratio, S_0, can be expressed as

$$S_0 = C_{rad}\, Z = \frac{P_T\, \pi^3\, G^2\, c\, \tau_0\, |K_c|^2\, \theta^2\, L_{sys}\, L_{atm}^2}{1024\times10^{18}\, \ln 2\, \lambda^2\, k\, T\, B\, r^2}\, Z \qquad (4)$$

where P_T is the transmitter peak power, λ is the radar wavelength, G is the antenna gain, c is the pulse propagation speed, τ_0 is the pulse duration, θ is the 3-dB antenna beamwidth, L_{sys} is the radar system loss, L_{atm} is the signal loss due to atmospheric absorption (cloud absorption is excluded), k is Boltzmann's constant, T is the system noise temperature, B is the receiver bandwidth, r is the radar range distance, $|K_c|^2$ is the dielectric factor of liquid water at 94 GHz, and Z is the equivalent cloud reflectivity factor (in mm^6/m^3). Both cloud signal and noise-only measurements will be collected. The noise component in the cloud signals, which on the average is equal to the noise-only measurements, will be removed at each range bin after appropriate signal averaging. We anticipate that the number of independent noise-only measurements collected will be much greater than that of the cloud signal measurements. As such, the effective cloud signal-to-noise ratio after averaging, S_I, can be expressed as:

$$S_I = \frac{<P_s>}{\sigma_s} \approx \frac{\sqrt{N_s}\, S_0}{S_0 + 1} = \frac{\sqrt{N_s}\, C_{rad}\, Z}{C_{rad}\, Z + 1} \qquad (5)$$

where N_s is the number of independent cloud measurements. By defining the minimum detectable cloud reflectivity, Z_{min}, as the cloud reflectivity value which gives rise to a unity signal-to-noise ratio after averaging, we have

$$Z_{min} = \frac{1}{(\sqrt{N_s} - 1)C_{rad}} \qquad (6)$$

To obtain better cloud detection sensitivity, the received pulses will be averaged along track; 1300 pulses will be averaged for 0.31 sec, equivalent to averaging over three instantaneous radar footprints. By using the radar parameters as listed in Table 1 and by assuming two-way atmospheric path losses of 1 dB in the upper atmosphere and 2 dB in the lower atmosphere, and $|K_c|^2$ - 0.8, the design yield Z_{min} values that are slight better than -30 dBZ. In Table 2 the preliminary estimates of the key performance characteristics are summarized.

Vertical resolution	500 m
Cross-track resolution	780 m
Along-track resolution (after pulse averaging)	2.3 km
Number of independent samples	1300
Minimum detectable dBZs:	
at altitude -20 km	-32.5 dBZ
at altitude - 400 m	-30.1 dBZ

Table 2. Preliminary performance estimates of the 94-GHz spaceborne cloud radar.

A block diagram of the proposed design is shown in Figure 3. The 3.33-μsec pulses are generated at 400 MHz and then up-converted to 94 GHz. These pulses are amplified by a solid-state amplifier driving the high-power extended interaction amplifier. This high-power signal is then sent to the antenna through a ferrite circulator. A three-junction ferrite transmit/receiver ("T/R") switch is used to protect the receiver. A small amount of power is coupled back to the receiver for transmit power calibration. During the receiver period, the received signal is sent through the circulator and the T/R switch to a 94-GHz low-noise amplifier. After that, the signal is filtered and down-converted to the first intermediate frequency. The signal is further amplified, filtered and converted to the second intermediate frequency, where it is sampled by the analog-to-digital converter and sent to the data system.

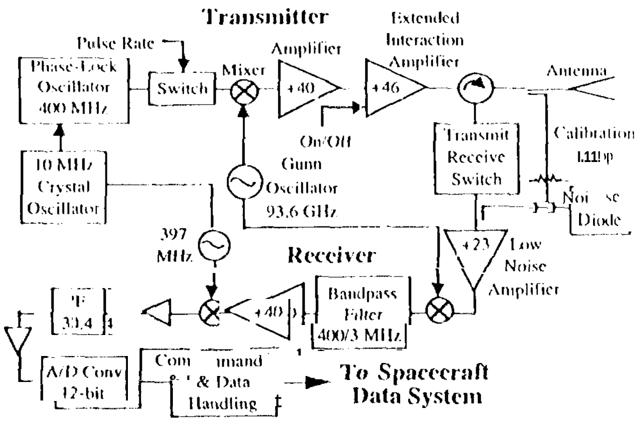

Figure 3. Strawman block diagram of the spaceborne cloud radar.

4. TECHNOLOGY ISSUES

A preliminary survey of the radar technology at 94 GHz has been made. The major technology development will be the space qualification of the 94-GHz EIA transmitter tube. Both ground-based and airborne 94-GHz EIAs, operating at or above the required peak power level, are currently available. However, since these devices are not designed for space application, developments to improve the EIA lifetime and to meet space qualification requirements are required.

5. AIRBORNE CLOUD RADAR

In order to test the spaceborne cloud radar design concept and equipment (e.g. EIA), and to develop and test algorithms for data analysis and interpretation, it is desirable to first develop an aircraft cloud radar. The aircraft instrument will have better sensitivity and spatial resolution to provide accurate data to assess the errors associated with the spaceborne radar retrieval algorithms. By incorporating Doppler capability, the aircraft instrument can also be used to study the cloud dynamics. For an airborne cloud radar, there are a number of additional design issues needed to be considered. In this section, we will briefly discuss two such issues: the wide dynamic range and Doppler/PRF selections.

Because of the downward viewing configuration, the radar echo profiles will include returns from both cloud and surface, we estimated that the maximum expected power is ~70 dB above the noise floor. This represents a wide dynamic range that must be accommodated by the RF, IF and digital portions of the radar receiver. A set of IF attenuation levels is needed in order to adjust the desired signal levels. The use of a 16-bit analog-to-digital converter appears to be adequate for this application.

For pulse radar operation, the maximum PRF is set to avoid range ambiguities. For Doppler measurements, however, the PRF should be large enough to avoid Doppler aliasing. For a radar operating on an aircraft moving at ~250 m/s, for instance, the PRF must be >32 KHz to avoid Doppler aliasing, which is obviously in conflicts with the desire to avoid range ambiguities. One potential approach to overcome this problem is by switching the PRF between two values that are both low enough to avoid range ambiguities. By properly choosing the PRF spacing, the aliased Doppler frequencies are different for the two PRFs. In this case, the maximum unambiguous Doppler range is determined by the least common multiple of the two PRFs (e.g., Li and Johnson, 1982).

6. SUMMARY

A strawman radar system design for cloud-profiling measurements from space was presented in this paper. In this design, the radar instrument operates at 94 GHz and at a nadir-pointing configuration. This strawman design is intended to serve as a benchmark in guiding the more vigorous future design and trade studies. The radar design is intended to be accommodated by a spacecraft with limited resources. It provides a vertical resolution of 500 m and a minimum detectable cloud reflectivity of slightly better than -30 dBZ.

This design uses the radar transmitter characteristics which are based on the existing airborne EIAs. For space application, improvements in the EIA lifetime and space qualification will be required. To support the development of a spaceborne cloud radar system, an aircraft cloud radar instrument is desirable. This instrument will test the space system design concept and technology and serve as a prelaunch development and testing of the data processing algorithms.

ACKNOWLEDGMENT

The research described in this paper was performed by the Jet Propulsion Laboratory, California Institute of Technology, under contract with the National Aeronautics and Space Administration.

REFERENCES

Atlas, D., "Advances in Radar Meteorology," *Adv. Geophys.*, vol. 10, 1964.

Li, F. and W. Johnson, "Ambiguities in spaceborne synthetic aperture radar systems," *IEEE Trans. Aerosp. & Elect. Sys.*, Vol. AES - 19, No. 3, 1983, pp. 389-397.

Tanner, A., S. L. Durden, R. Denning, E. Im, F. K. Li, W. Ricketts, and W. Wilson, "Pulse compression with very low sidelobes in an airborne rain mapping radar," *IEEE Trans. Geosci. & Remote Sensing*, in press,

Ulaby, F. T., and M. C. Dobson, *Handbook of Radar Scattering Statistics for Terrain*, Artech House, Boston, MA., 1998

Ulaby, F. T., R. K. Moore, and A. K. Fung, *Microwave Remote Sensing Active and Passive, Volume II*, Addison-Wesley, Reading, MA., 1982.

World Climate Research Program, *Utility and Feasibility of a Cloud Profiling Radar*, WCRP-84, Pasadena, CA, June 29 - July 1, 1993.